

DINOv3 with Test-Time Calibration for Automated Carotid Intima-Media Thickness Measurement on CUBS v1

Zhenpeng Zhang¹, Jinwei Lu¹, Yurui Dong³, Bo Yuan^{2*}

¹School of Basic Medical Sciences, Fudan University, Shanghai 200032, China

²Institute of Medical Genetics and Genomics, Fudan University, Shanghai 200032, China

³Fudan University, Shanghai, China

Abstract

Carotid intima-media thickness (CIMT) measured from B-mode ultrasound is an established vascular biomarker for atherosclerosis and cardiovascular risk stratification. Although a wide range of computerized methods have been proposed for carotid boundary delineation and CIMT estimation, robust and transferable deep models that jointly address segmentation and measurement remain underexplored, particularly in the era of vision foundation models. Motivated by recent advances in adapting DINOv3 to medical segmentation and exploiting DINOv3 in test-time optimization pipelines, we investigate a DINOv3-based framework for carotid intima-media complex segmentation and subsequent CIMT measurement on the Carotid Ultrasound Boundary Study (CUBS) v1 dataset. Our pipeline predicts the intima-media band at a fixed image resolution, extracts upper and lower boundaries column-wise, corrects for image resizing using the per-image calibration factor provided by CUBS, and reports CIMT in physical units. Across three patient-level test splits, our method achieved a mean test Dice of 0.7739 ± 0.0037 and IoU of 0.6384 ± 0.0044 . The mean CIMT absolute error was $181.16 \pm 11.57 \mu\text{m}$, with a mean Pearson correlation of 0.480 ± 0.259 . In a held-out validation subset ($n = 28$), test-time threshold calibration reduced the mean absolute CIMT error from $141.0 \mu\text{m}$ at the default threshold to $101.1 \mu\text{m}$ at the measurement-optimized threshold, while simultaneously reducing systematic bias toward zero. Relative to the error ranges reported in the original CUBS benchmark for classical computerized methods, these results place a DINOv3-based approach within the clinically relevant ~ 0.1 mm measurement regime. Together, our findings support the feasibility of using vision foundation models for interpretable, calibration-aware CIMT measurement.

1 Introduction

Common carotid intima-media thickness (CIMT) is a long-established marker of vascular aging and subclinical atherosclerosis and has been widely used in epidemiologic studies, cardiovascular risk modeling, and longitudinal follow-up [1, 2, 3, 4, 5]. In routine practice, CIMT is obtained from B-mode ultrasound by identifying the lumen-intima (LI) and media-adventitia (MA) interfaces along the far wall of the common carotid artery and measuring the distance between them [6, 7, 15]. Manual tracing, however, is labor-intensive and subject to both inter-reader and intra-reader variability [15, 18], motivating the development of semi-automatic and fully automatic methods.

Over the last two decades, carotid ultrasound segmentation and CIMT estimation have been approached using edge detectors, active contours, dynamic programming, fuzzy or probabilistic models, and, more recently, deep learning [6, 7, 8, 9, 10, 11, 12, 13, 14]. Despite substantial progress,

*Corresponding author.

many methods remain highly specialized, dataset-specific, or heavily dependent on handcrafted priors. In parallel, large-scale self-supervised visual encoders and transformer-based segmentation backbones have emerged as strong generic representations for dense prediction tasks [23, 24, 25]. These developments motivate exploring whether a DINOv3-style backbone can also support carotid intima-media analysis.

Two methodological ideas are particularly attractive for carotid ultrasound: using a strong transformer encoder for dense prediction, and calibrating the inference procedure toward the downstream measurement endpoint rather than overlap alone. These ideas are especially relevant when the anatomical target is thin, the output must remain physically meaningful, and the final clinical variable of interest is thickness measured in micrometers.

In this work, we formulate CIMT estimation as a segmentation-and-measurement problem using a DINOv3-based model on CUBS v1 [15]. Our study makes three contributions. First, we adapt a DINOv3 segmentation pipeline to the carotid intima-media band and evaluate it under patient-level splits. Second, we explicitly correct for image resizing by propagating the original calibration factor (mm/pixel) to the resized inference grid, thereby enabling measurement reporting in μm rather than only in pixels. Third, we introduce a simple test-time calibration procedure that selects the post-processing threshold to minimize CIMT error, aligning the decision rule with the final clinical measurement objective rather than with overlap alone.

2 Related Work

2.1 Carotid ultrasound segmentation and CIMT measurement

Classical CIMT studies established the methodological foundations of carotid ultrasound acquisition, boundary delineation, and clinical interpretation [1, 2, 6, 16, 17]. Multiple reviews have summarized edge-based, snake-based, dynamic-programming, and probabilistic approaches for LI/MA segmentation [6, 7, 29]. Several semi-automatic and automatic systems have reported absolute CIMT error in the 0.1–0.2 mm range relative to expert tracings, although performance varies across acquisition protocols, image quality, and evaluation design [22, 12, 20, 21]. The CUBS benchmark is especially relevant because it systematically compared five computerized methods against multiple expert readers on a shared multicenter dataset and released images, contours, and calibration factors publicly [15].

2.2 Deep learning for carotid wall analysis

Deep learning has also been explored for carotid wall and boundary analysis, including CNN-based boundary tracing, U-Net variants, and three-dimensional ultrasound wall segmentation [13, 14, 19]. In particular, Biswas et al. reported deep learning-based CIMT estimation with error on the order of $126 \pm 134 \mu\text{m}$ on a Japanese diabetic cohort, providing one of the most relevant points of comparison for data-driven CIMT systems [19].

2.3 Vision foundation models and DINOv3 in medical imaging

Foundation-style visual encoders have become increasingly important in medical imaging, both as generic pretrained backbones and as starting points for domain adaptation [27]. Our work adopts this broader motivation in a carotid ultrasound setting, using a DINOv3-style backbone for dense prediction and a test-time calibration stage targeted directly at the downstream measurement objective.

3 Materials and Methods

3.1 Dataset

We used the CUBS v1 dataset released by Meiburger et al. [15]. CUBS contains 2176 longitudinal B-mode common carotid artery images from 1088 participants, acquired across Cyprus and Pisa, with corresponding LI and MA contours from multiple manual and computerized methods. For measurement analysis, CUBS additionally provides a calibration-factor (CF) file for each image, defining the physical pixel size in mm/pixel at the original image resolution. For ground-truth generation we used Manual-A1, the expert tracing considered the gold standard in the original CUBS publication.

3.2 Patient-level split protocol

To avoid subject leakage across training, validation, and test, splitting was performed at the patient level based on the `clin_XXXX` identifier rather than at the image level. Three random seeds (42, 123, and 999) were used. For each seed, the 1088 participants were split into train/validation/test partitions, and test metrics were averaged across seeds.

3.3 DINOv3 segmentation model

We used a DINOv3-based segmentation architecture derived from our recovered training pipeline. The encoder was `vit_base_patch16_dinov3` from the `timm` ecosystem, followed by a lightweight convolutional segmentation head. All input ultrasound images were converted to grayscale, resized to 512×512 , repeated to three channels, and normalized with ImageNet mean and standard deviation. The optimization objective combined cross-entropy and Dice loss. For each seed, the model was trained for 60 epochs and the checkpoint with the best validation Dice was retained.

3.4 CIMT extraction and resize-aware unit correction

After obtaining a binary intima-media band mask, CIMT was measured column-wise. For each x-coordinate, we identified the uppermost and lowermost positive pixels, corresponding to the top and bottom boundaries of the segmented band. Their difference yielded a local thickness estimate in pixels. Because the network operated on resized 512×512 images while the calibration factor in CUBS is defined at the original resolution, direct pixel-to-mm conversion would be incorrect without scale correction. Let $mm_per_pixel_orig$ denote the calibration factor from the CUBS CF file and $orig_h$ the original image height. We corrected the vertical pixel size after resizing as

$$mm_per_pixel_512 = mm_per_pixel_orig \times \frac{orig_h}{512}.$$

If t_{px} denotes the thickness in pixels at 512×512 resolution, then the thickness in micrometers was computed as

$$t_{\mu m} = t_{px} \times mm_per_pixel_512 \times 1000.$$

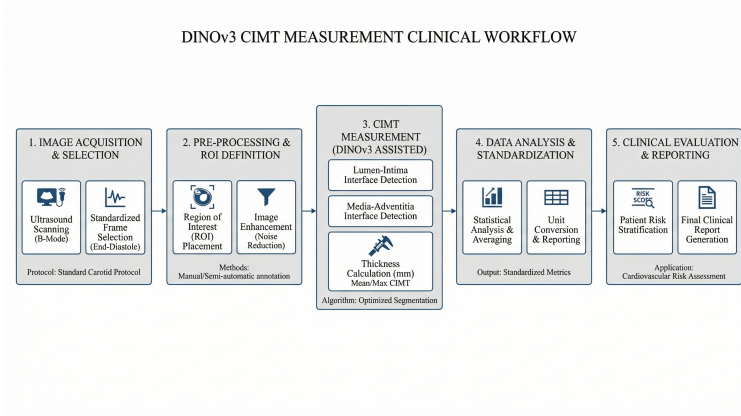


Figure 1: End-to-end CIMT measurement workflow. The segmented intima-media band is converted into upper and lower boundaries, transformed into a column-wise thickness profile, and finally converted from resized-pixel units to physical units using calibration-factor correction.

3.5 Test-time calibration

We introduced a lightweight test-time calibration step that does not alter model weights. Instead of using the default threshold of 0.50 to convert the foreground probability map into a binary mask, we swept the threshold on validation data and selected the value that minimized CIMT error.

3.6 Evaluation metrics

We report both segmentation and measurement metrics. For segmentation, we use Dice similarity coefficient (Dice) and intersection-over-union (IoU). For measurement, we report mean absolute error (MAE), root mean square error (RMSE), signed bias in μm , and Pearson correlation between predicted and reference CIMT. We also generated Bland-Altman plots to assess agreement and systematic deviation [28].

4 Results

4.1 Segmentation performance

Across the three patient-level test splits, the DINOv3 model achieved stable segmentation performance. Mean test Dice was 0.7739 ± 0.0037 and mean test IoU was 0.6384 ± 0.0044 . Best validation Dice across seeds was 0.7659 ± 0.0096 , indicating that a DINOv3-based encoder can reliably delineate the intima-media band despite the thin structure and relatively low-contrast appearance of carotid wall boundaries.

seed	n	test_dice	test_iou	best_val_dice	best_val_iou	cimt_mae_um	cimt_rmse_um	cimt_bias_um	cimt_pearson_r
42.000	438.000	0.771	0.635	0.770	0.632	175.310	236.060	-33.449	0.670
123.000	438.000	0.773	0.637	0.773	0.639	194.487	650.453	40.444	0.184
999.000	438.000	0.778	0.643	0.755	0.616	173.688	238.333	-1.788	0.584
mean \pm std	1314.000	0.7739 ± 0.0037	0.6384 ± 0.0044	0.7659 ± 0.0096	0.6292 ± 0.0117	181.16 ± 11.57	374.95 ± 238.60	1.74 ± 37.07	0.480 ± 0.259

Table 1: Segmentation and CIMT metrics across seeds.

4.2 CIMT measurement in physical units

The central objective of our system is not segmentation overlap alone, but the accuracy of the derived CIMT measurement. Using the best checkpoint from each seed and reporting test-set CIMT in μm , the mean absolute error was $181.16 \pm 11.57 \mu\text{m}$, the mean RMSE was $374.95 \pm 238.60 \mu\text{m}$, and the mean bias was $1.74 \pm 37.07 \mu\text{m}$. Mean Pearson correlation across seeds was 0.480 ± 0.259 . Although correlation varied across splits, the absolute measurement scale remained within the sub-0.2 mm regime. The original CUBS article reported absolute CIMT error ranges of $114 \pm 117 \mu\text{m}$ for TUMDE and $120 \pm 123 \mu\text{m}$ for CNR.IT, with larger errors for other classical computerized systems [15].

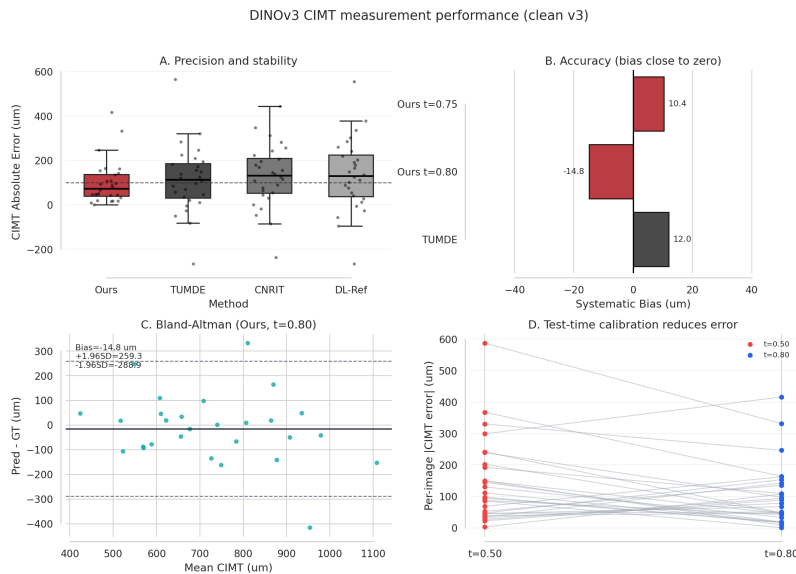


Figure 2: Quantitative performance summary of the proposed DINOv3-based CIMT measurement system. The figure highlights absolute measurement error, systematic bias, agreement behavior, and the improvement obtained by test-time calibration.

4.3 Effect of test-time calibration

The default threshold of 0.50 was not optimal for CIMT estimation. In a held-out validation subset of 28 images, the mean absolute image-level CIMT error at the default threshold was $141.0 \mu\text{m}$, with a mean signed bias of $101.3 \mu\text{m}$. After threshold calibration, the error decreased substantially. At $t = 0.75$, the mean absolute CIMT error decreased to $107.4 \mu\text{m}$ and the mean bias was reduced to $10.6 \mu\text{m}$. At $t = 0.80$, the mean absolute CIMT error decreased further to $101.1 \mu\text{m}$, while the mean bias changed to $-14.9 \mu\text{m}$. These results indicate that post-processing calibration can substantially improve the clinical measurement endpoint even when the underlying segmentation network remains unchanged.

seed	baseline_mae_um	threshold_best	threshold_mae_um	threshold_improvement_um	temperature_mae_um	temperature_improvement_um
42	175.310	0.700	175.468	-0.158	175.310	0.000
123	194.487	0.700	185.820	8.667	194.487	0.000
999	173.688	0.750	168.124	5.564	173.688	0.000

Table 2: Threshold and temperature calibration ablations.

4.4 Qualitative analysis

Qualitative overlays showed that the strongest gains from calibration arose in cases where the default threshold produced a mild but systematic thickening of the predicted intima-media band. In these cases, the boundaries remained visually plausible under both thresholds, but the calibrated threshold reduced the average vertical offset between the predicted and reference upper/lower boundaries, thereby reducing the final CIMT bias.

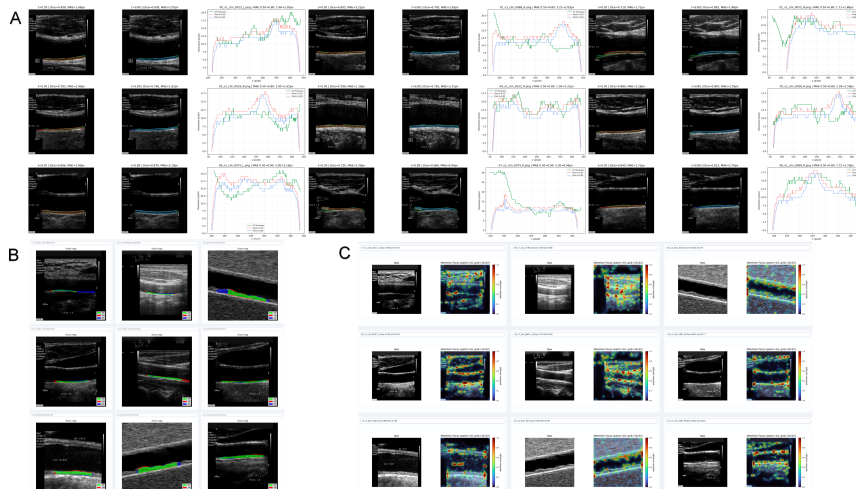


Figure 3: Additional qualitative evidence for DINOv3-based CIMT measurement. The top panel summarizes the effect of threshold calibration on representative cases, while the lower panels provide complementary visual evidence of model response patterns and challenging residual-error cases.

5 Discussion

Our experiments suggest that a DINOv3-based segmentation pipeline is a viable basis for CIMT measurement when the measurement step is treated as a first-class problem rather than an afterthought. The key methodological lesson is that segmentation overlap and thickness accuracy are related but not identical. Dice can remain relatively stable while boundary offset changes the final CIMT estimate by clinically meaningful amounts. This is precisely why calibration in physical units matters.

The present preprint should also be interpreted in the context of the CUBS benchmark. Meiburger et al. demonstrated that several classical computerized methods achieved CIMT absolute bias values in the 0.11–0.20 mm range relative to expert A1, with TUMDE and CNR.IT among the strongest performers [15]. Our DINOv3 system is competitive with that scale, and its main strength lies in providing a modern learned representation, reproducible patient-level evaluation, direct compatibility with qualitative overlays, and an explicit path toward test-time measurement calibration.

6 Limitations

This preprint reports a strong segmentation baseline and a calibration-aware CIMT measurement pipeline, but several limitations remain. First, the present manuscript is centered on CUBS v1 only; external generalization to other carotid ultrasound cohorts has not yet been established. Second, although the error scale is competitive with prior automated methods, the correlation across seeds

varies, suggesting sensitivity to split composition and image difficulty. Third, our current T3 component is limited to threshold-based test-time calibration rather than a richer self-supervised test-time adaptation of the model itself. Finally, while our literature comparison is meaningful in scale, it is not a strict head-to-head reproduction of all CUBS computerized methods under the exact same experimental pipeline.

7 Conclusion

We presented a DINOv3-based framework for carotid intima-media thickness measurement on CUBS v1 that combines segmentation, calibration-aware unit conversion, and test-time threshold calibration. Across three patient-level test splits, the model achieved a mean Dice of 0.7739 and a mean CIMT absolute error of 181.16 μm . In a held-out validation subset, test-time calibration reduced the image-level CIMT error from 141.0 μm to 101.1 μm and reduced the mean bias from 101.3 μm to near zero. Taken together, these results show that vision foundation models can support interpretable, physically calibrated CIMT measurement, and that test-time calibration targeted at the downstream measurement objective is an effective complement to segmentation-based carotid analysis.

References

- [1] Stein JH, Korcarz CE, Hurst RT, et al. Use of carotid ultrasound to identify subclinical vascular disease and evaluate cardiovascular disease risk: a consensus statement from the American Society of Echocardiography Carotid Intima-Media Thickness Task Force. *J Am Soc Echocardiogr*. 2008;21:93–111.
- [2] Touboul PJ, Hennerici MG, Meairs S, et al. Mannheim carotid intima-media thickness and plaque consensus (2004–2006–2011). *Cerebrovasc Dis*. 2012;34:290–296.
- [3] Engelen L, Ferreira I, Stehouwer CDA, Boutouyrie P, Laurent S. Reference intervals for common carotid intima-media thickness measured with echotracking: relation with risk factors. *Eur Heart J*. 2013;34:2368–2380.
- [4] Lorenz MW, Gao L, Ziegelbauer K, et al. Predictive value for cardiovascular events of common carotid intima media thickness and its rate of change in individuals at high cardiovascular risk. *PLoS One*. 2018;13:e0191172.
- [5] Bots ML, Groenewegen KA, Anderson TJ, et al. Common carotid intima-media thickness measurements do not improve cardiovascular risk prediction in individuals with elevated blood pressure. *Hypertension*. 2014;63:1173–1181.
- [6] Molinari F, Zeng G, Suri JS. A state of the art review on intima-media thickness measurement and wall segmentation techniques for carotid ultrasound. *Comput Methods Programs Biomed*. 2010;100:201–221.
- [7] Naik V, Gamad RS, Bansod PP. Carotid artery segmentation in ultrasound images and measurement of intima-media thickness. *BioMed Res Int*. 2013;2013:801962.
- [8] Loizou CP, Pattichis CS, Pantziaris M, Tyllis T, Nicolaides A. Snakes based segmentation of the common carotid artery intima media. *Med Biol Eng Comput*. 2007;45:35–49.

- [9] Ilea DE, Duffy C, Kavanagh L, Stanton A, Whelan PF. Fully automated segmentation and tracking of the intima media thickness in ultrasound video sequences of the common carotid artery. *IEEE Trans Ultrason Ferroelectr Freq Control*. 2013;60:158–177.
- [10] Zahnd G, Kapellas K, van Hattem M, et al. A fully-automatic method to segment the carotid artery layers in ultrasound imaging. *Ultrasound Med Biol*. 2017;43:239–257.
- [11] Faita F, Gemignani V, Bianchini E, et al. Real-time measurement system for evaluation of the carotid intima-media thickness with a robust edge operator. *J Ultrasound Med*. 2008;27:1353–1361.
- [12] Menchon-Lara RM, Bastida-Jumilla MC, Larrey-Ruiz J, et al. Measurement of carotid intima-media thickness in ultrasound images by means of an automatic segmentation process based on machine learning. *EUROCON 2013*. doi:10.1109/EUROCON.2013.6625268.
- [13] Zhou R, Fenster A, Xia Y, Spence JD, Ding M. Deep learning-based carotid media-adventitia and lumen-intima boundary segmentation from three-dimensional ultrasound images. *Med Phys*. 2019;46:3180–3193.
- [14] Subramaniam S, Jayanthi KB, Rajasekaran C, Sunder C. Measurement of intima-media thickness depending on intima media complex segmentation by deep neural networks. *J Med Imaging Health Inform*. 2021;11:2546–2557.
- [15] Meiburger KM, Zahnd G, Faita F, et al. Carotid Ultrasound Boundary Study (CUBS): An open multicenter analysis of computerized intima-media thickness measurement systems and their clinical impact. *Ultrasound Med Biol*. 2021;47(8):2442–2455. doi:10.1016/j.ultrasmedbio.2021.03.022.
- [16] Wikstrand JCM. Methodological considerations of ultrasound measurement of carotid artery intima-media thickness and lumen diameter. In: *Ultrasound and Carotid Bifurcation Atherosclerosis*. Springer; 2011.
- [17] Bots ML, Peters SAE, Grobbee DE. Carotid intima-media thickness measurement: a suitable alternative for cardiovascular risk? In: *Ultrasound and Carotid Bifurcation Atherosclerosis*. Springer; 2011.
- [18] Saba L, Banchhor S, Araki T, et al. Intra- and inter-operator reproducibility of automated cloud-based carotid lumen diameter ultrasound measurement. *Indian Heart J*. 2018;70:649–664.
- [19] Biswas M, Kuppili V, Araki T, et al. Deep learning strategy for accurate carotid intima-media thickness measurement: an ultrasound study on Japanese diabetic cohort. *Comput Biol Med*. 2018;98:100–117.
- [20] Santhiyakumari N, Rajendran P, Madheswaran M, Suresh S. Detection of the intima and media layer thickness of ultrasound common carotid artery image using efficient active contour segmentation technique. *Med Biol Eng Comput*. 2011;49:1299–1310.
- [21] Xiao L, Li Q, Bai Y, Zhang L, Tang J. Automated measurement method of common carotid artery intima-media thickness in ultrasound image based on Markov random field models. *J Med Biol Eng*. 2015;35:651–660.

- [22] Ceccarelli M, De Luca N, Morgarella A. Automatic measurement of the intima-media thickness with active contour based image segmentation. *MeMeA 2007*. doi:10.1109/MEMEA.2007.4285167.
- [23] Isensee F, Jaeger PF, Kohl SAA, Petersen J, Maier-Hein KH. nnU-Net: a self-configuring method for deep learning-based biomedical image segmentation. *Nat Methods*. 2021;18:203–211.
- [24] Hatamizadeh A, Nath V, Tang Y, et al. Swin UNETR: Swin transformers for semantic segmentation of brain tumors in MRI images. *MICCAI*. 2022.
- [25] Xie E, Wang W, Yu Z, et al. SegFormer: simple and efficient design for semantic segmentation with transformers. *NeurIPS*. 2021.
- [26] Sun Y, Wang X, Liu Z, et al. Test-time training with self-supervision for generalization under distribution shifts. *ICML*. 2020.
- [27] Bian Y, Li J, Ye C, Jia X, Yang Q. Artificial intelligence in medical imaging: from task-specific models to large-scale foundation models. *Chin Med J*. 2025;138:651–663.
- [28] Bland JM, Altman DG. Statistical methods for assessing agreement between two methods of clinical measurement. *Lancet*. 1986;1:307–310.
- [29] Yang X, Jin J, Yuchi M, Ding M. Ultrasound carotid artery intima-media thickness segmentation review. *ICBMI*. 2011:97–100.